Journal of Materials Chemistry C

ROYAL SOCIETY OF CHEMISTRY

COMMUNICATION

View Article Online
View Journal | View Issue

Open Access Article. Published on 23 March 2022. Downloaded on 4/14/2022 6:29:34 PM.
This article is licensed under a Creative Commons Attribution-NonCommercial 3.0 Unported Licence.

Cite this: *J. Mater. Chem. C*, 2022, **10**, 5783

Received 12th January 2022,
Accepted 22nd March 2022

DOI: 10.1039/d2tc00179a

rsc.li/materials-c

Elucidating the electronic properties of single-wall carbon nanohorns†

Anna Zieleniewska, [a] Fabian Lodermeyer, [b] Maurizio Prato, [cde] Garry Rumbles, [af] Dirk M. Guldi [b] and Jeffrey L. Blackburn *[a]

Single-walled carbon nanohorns are an allotrope of carbon with promising properties for a variety of applications. Despite their promise, the majority carrier type (*i.e.* electrons or holes) that defines the electronic properties of this novel semiconductor is poorly understood and so far only indirect measurements have been employed to arrive at contradictory results. Here, we directly determine the majority carrier type in single-wall carbon nanohorns for the first time by means of thermopower measurements. Using this direct method, we show that SWCNH films exhibit a positive Seebeck coefficient indicating that SWCNHs behave as p-type semiconductors. This result is further corroborated by intentionally tuning the hole or electron concentrations of SWCNH layers *via* redox doping with molecular electron acceptors and donors, respectively. These results provide a framework for both measuring and chemically tuning the majority carrier type in this emerging nanocarbon semiconductor.

Introduction

Single-wall carbon nanohorns (SWCNHs) are an emerging class of semiconducting nanocarbons with several important differences from their close relatives, single-wall carbon nanotubes (SWCNTs). SWCNHs are conical structures with a sharp apical angle of 20°.[1] A single carbon nanohorn is 2–5 nm in diameter and 40–50 nm in length and individual nanohorns tend to associate into loosely bound aggregates of 100 nm diameter.[2] SWCNHs can be synthesized on a large scale by a metal catalyst-free CO_2 laser ablation process,[3,4] making them easily accessible to a variety of technological fields. They have been studied, *e.g.*, in drug delivery systems,[5–7] photothermal therapy,[8] catalysis,[9,10] gas storage,[11] and photovoltaics.[12] In particular, SWCNHs have been used in photoinduced electron-transfer processes,[13] for efficient dye-sensitized solar cells,[14–16] and as active components for the reduction of CO_2 to formic acid,[17] or for O_2 reduction to H_2O_2.[18,19]

In all these very promising applications SWCNHs play a significant role in electron transport, enhancing charge separation states and catalytic performances, but it is not yet clear what is the role of SWCNHs in these devices, whether n-type or p-type semiconductors. Majority carrier type is a tunable material property that impacts ground-state electronic properties, excited-state dynamics, and the ultimate functionality of semiconductors in a broad array of devices. To date, literature reports have only used indirect gas adsorption methods to infer the majority carrier type and electronic properties of pristine SWCNHs and the results have been contradictory. Kaneko *et al.* suggested that SWCNHs behave as n-type semiconductors,[20] since exposure of compressed SWCNH pellets to O_2 molecules (considered to be electron acceptors) decreased the electrical conductivity, while adsorption of relatively reducing CO_2 molecules (considered to be electron donors) increased the conductivity. In contrast, Suehiro *et al.* found that the conductance of SWCNHs increased or decreased upon exposure to relatively oxidizing NO_2 molecules or reducing NH_3 molecules, respectively.[21] They therefore concluded that SWCNHs, similar to most reports on SWCNT transport in ambient conditions, behave as p-type semiconductors. There is thus no consensus on the electronic properties of SWCNHs and no direct methods have been used thus far to elucidate majority carrier type in SWCNHs.

[a] *Chemistry and Nanoscience Center, National Renewable Energy Laboratory, Golden, CO 80401, USA. E-mail: Jeffrey.blackburn@nrel.gov*
[b] *Department of Chemistry and Pharmacy & Interdisciplinary Center for Molecular Materials, Friedrich-Alexander-Universität Erlangen-Nürnberg, Egerlandstr. 3, 91058 Erlangen, Germany*
[c] *Center of Excellence for Nanostructured Materials, INSTM, Unit of Trieste, Dipartimento di Scienze Chimiche e Farmaceutiche, Università degli Studi di Trieste, Piazzale Europa 1, 34127 Trieste, Italy*
[d] *Centre for Cooperative Research in Biomaterials (CIC BiomaGUNE), Basque Research and Technology Alliance (BRTA), Paseo de Miramón 194, Donostia-San Sebastián 20014, Spain*
[e] *Ikerbasque, Basque Foundation for Science, Bilbao 48013, Spain*
[f] *Renewable and Sustainable Energy Institute, University of Colorado Boulder, Boulder, Colorado 80309, USA*

† Electronic supplementary information (ESI) available. See DOI: 10.1039/d2tc00179a

Open Access Article. Published on 23 March 2022. Downloaded on 4/14/2022 6:29:34 PM.
This article is licensed under a Creative Commons Attribution-NonCommercial 3.0 Unported Licence.

In the light of the current discrepancy in the literature, we set out to address the simple outstanding question: Do SWCNHs behave as n-type or p-type semiconductors and can this behavior be tuned? Instead of using indirect gas adsorption measurements, we chose to pursue thermopower (Seebeck coefficient) measurements as a direct probe of the majority carrier type. The Seebeck coefficient, with units of V K^{-1}, reflects the voltage produced in a semiconductor when it is subjected to a thermal gradient. This thermopower voltage is produced by the net flow of electronic charge carriers (electrons or holes) from the hot side of the semiconductor to the cold side of the semiconductor. As charge carriers build up on either side of the semiconductor, they establish a voltage that opposes the thermal drift of carriers, and the sign of this voltage is a direct indicator of the majority carrier type present in the semiconductor. While majority carrier type is often inferred from field-effect transistor (FET) measurements, the conduction type measured in an FET depends on both the intrinsic material properties and the injection barriers at the electrode/material interface.[22] In contrast, the Seebeck effect is a fundamental process that is dictated by the impact of entropy on charge carriers within the material. By definition, majority electrons in an n-type semiconductor produce a negative Seebeck coefficient, while majority holes in a p-type semiconductor produce a positive Seebeck coefficient.[23] Despite being applied extensively to other nanocarbon semiconductors and semiconducting polymers,[24] this simple method has surprisingly not yet been employed in the literature to provide a clear depiction of SWCNH electronic properties.

In the following study, we unambiguously demonstrate that as-prepared SWCNHs are p-type semiconductors with positive Seebeck coefficients. We also show that the majority carrier type and density can be tuned, with molecular redox dopants, to encompass a range of both p-type and n-type transport. These results elucidate a simple methodology that can be used to correlate SWCNH electronic properties with device functionality, a key practice for developing and optimizing optoelectronic technologies.

In this study, we synthesize SWCNHs by a CO_2 laser ablation technique.[25] The quality of SWCNHs used in this work was confirmed with transmission electron microscopy (TEM) and Raman measurements. Fig. 1a shows a characteristic TEM image of SWCNHs that are aggregated into 'dahlia'-shaped bundles that are *ca.* 100 nm in diameter. Fig. 1b shows the Raman spectrum of as-grown SWCNHs with an excitation wavelength of 532 nm. Two pronounced bands are observed at 1333 and 1594 cm^{-1}, which are assigned to the D and G band, respectively.[26] The latter arises from a symmetric E_{2g} mode at the Γ point (G mode) in the Brillouin zone that arises from in-plane stretching of adjacent C–C bonds in sp^2-carbon materials.[27,28] The former corresponds to a A_{1g} symmetry (D mode) introduced by intervalley scattering at defects or edges.[30] The I_D/I_G ratio in Fig. 1b is 1.40, in line with the typical ratio observed for SWCNH samples.[12,29] The second-order overtone of the D band, namely the 2D band,[31] is also observed at *ca.* 2700 cm^{-1}.

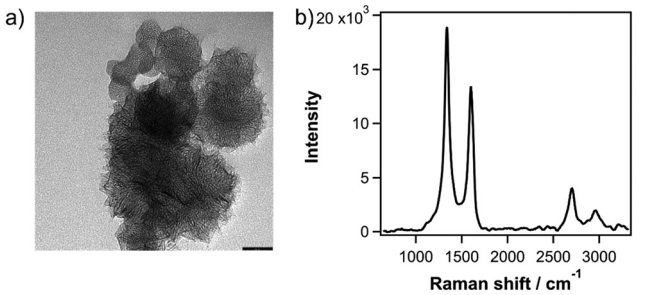

Fig. 1 (a) TEM image of dahlia-shaped SWCNH bundles. Scale bar is 50 nm. (b) Raman spectra of SWCNHs, excited with a 532 nm laser.

For transport measurements, thin films of pristine SWCNHs were produced by spin-coating a SWCNH dispersion (3.6 μg $μL^{-1}$ in *ortho*-dichlorobenzene) onto glass substrates. Sheet resistance was measured by four-point probe and film thicknesses were measured by profilometry. The sheet resistivity sharply reduces from 49.11 to 0.27 Ω cm^{-1} for layer thicknesses of *ca.* 110 and 370 nm, respectively. With a further increase in layer thickness the resistance only decreases slightly. Hence, substrates with layer thicknesses of *ca.* 370 nm were used for measuring the Seebeck coefficients. Seebeck coefficients were measured on a home-built method-of-four-coefficients system, with pressed indium pads for making contact to copper heater blocks, as previously described.[32,40] As presented in Fig. 2a, pristine SWCNHs films show a positive Seebeck coefficient of +42.9 μV K^{-1}, thus indicating that SWCNHs behave as p-type semiconductors.

To confirm the robustness of the measurement and of the SWCNH electrical properties, we performed two experiments. First, since oxygen adsorption and desorption has been shown to change the majority carrier type and Seebeck sign in other π-conjugated semiconductors such as SWCNTs,[33] we measured a SWCNH film under vacuum as a function of time to exclude possible impact of the environmental conditions, *i.e.* oxygen and air humidity. Similar to the measurements under ambient conditions, the Seebeck coefficient remained positive with

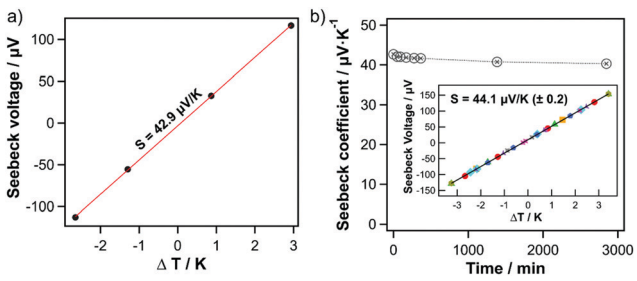

Fig. 2 (a) Seebeck voltage as a function of temperature difference under ambient conditions. The Seebeck coefficient is determined from the slope of the linear fit. (b) The Seebeck coefficient as a function of time under vacuum. Inset: Seebeck voltage for a series of consecutive cycles with different sets of ΔT values. The black line is a linear regression fit to the combined data from all nine experiments. The Seebeck coefficient shown is the average value and standard deviation from the nine separate measurements.

 This journal is © The Royal Society of Chemistry 2022

Open Access Article. Published on 23 March 2022. Downloaded on 4/14/2022 6:29:34 PM.
This article is licensed under a Creative Commons Attribution-NonCommercial 3.0 Unported Licence.

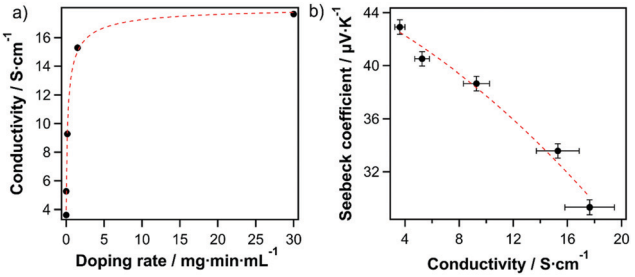

Fig. 3 (a) Conductivity of SWCNHs as a function of OA doping rate. (b) The Seebeck coefficient as a function of conductivity upon OA doping. The lines serve as a guide to the eye.

minor changes (ΔS = 2 μV K^{-1}) under vacuum for two days (Fig. 2b). Second, reproducibility of the data was confirmed by measuring a series of consecutive cycles with different sets of ΔT values. The inset of Fig. 2b shows nine separate experimental runs, where each color/symbol combination is a different measurement, and the black line shows a linear regression to the combined data from all nine experiments. This comparison clearly demonstrates that (1) the Seebeck voltage is linear with respect to ΔT, regardless of the range (up to $\Delta T = \pm 3$ K) and/or exact values of ΔT, and (2) the measurement is extremely repeatable over many cycles.

To further confirm this finding, and to demonstrate further tunability of the majority carrier type/density, we doped SWCNHs either n-type or p-type by submersion into a solution of an appropriate molecular redox dopant. Treatment of films with the one-electron oxidant triethyloxonium hexachloroantimonate (OA)[34] increased the sheet conductivity of the pristine SWCNH-based layer 3.57 S cm^{-1} to a value of 16.67 S cm^{-1} or the highly doped film, due to an increase in charge carrier density (Fig. 3a). The doping level can be modified either by varying concentrations and/or the exposure duration (Fig. 3a and Table S1, ESI†). The charge carrier type is confirmed as holes by Seebeck measurements (Fig. 3b) and an increase in hole concentration is accompanied by a decrease in the Seebeck coefficient. The injection of hole majority carriers into SWCNHs by OA is consistent with numerous previous reports on semiconducting SWCNTs (s-SWCNTs).[35,36] Furthermore, the anti-correlated conductivity and Seebeck coefficient are in good agreement with their direct and inverse dependences, respectively, on carrier concentration.[37,38] Thus, the predictable and tunable behavior observed for OA doping confirms our finding of the pristine SWCNHs acting as a p-type semiconductor.

Despite being p-type conductors in their as-prepared state, many nanocarbon materials such as SWCNTs can be doped appropriately to display n-type conductivity.[36] In an attempt to produce n-type SWCNHs, we doped SWCNH thin films with bis(pentamethylcyclopentadienyl) cobalt(II) (decamethylcobaltocene), a strong reductant with a one-electron redox potential of −1.94 V *vs.* ferrocene/ferrocenium.[39] Immersing the SWCNH film in this strong n-dopant shifted the Seebeck coefficient to a negative value of −41.22 μV K^{-1}, confirming that the dopant injects electron majority carriers into the SWCNHs. Once an n-type doped film is exposed to air, the Seebeck coefficient changes to −29.6 μV K^{-1} after 48 hours. Interestingly, the n-type conductivity of SWCNHs is more stable than that observed for s-SWCNTs, where the negative thermopower decays within minutes unless the SWCNT film is appropriately encapsulated to prevent electron compensation by oxygen.[36] This intriguing difference may arise from differences in chemical potentials for electrons in the lowest conduction levels of SWCNHs and s-SWCNTs, especially with respect to the reduction potential of oxygen.

In conclusion, our study demonstrates that pristine SWCNHs films exhibit a positive Seebeck coefficient indicating that SWCNHs behave as p-type semiconductors. Additionally, further p-doping of the SWCNH layers lead to a decrease of the Seebeck coefficient due to an increase in the hole carrier concentration and electron injection from strongly reducing molecules converts the SWCNHs to n-type. Altogether, our results point to the p-type character of pristine SWCNHs and resolves the contradictory conclusions arising from prior indirect gas adsorption methods.

Conflicts of interest

There are no conflicts to declare.

Acknowledgements

This work was authored, in part, by the National Renewable Energy Laboratory, operated by Alliance for Sustainable Energy, LLC, for the U.S. Department of Energy (DOE) under Contract No. DE-AC36-08GO28308. Transport and spectroscopic measurements were conducted as part of the Solar Photochemistry Program of the Chemical Sciences, Geosciences, & Biosciences (CSGB) Division at the U.S. DOE Office of Science: Basic Energy Sciences. The views expressed in the article do not necessarily represent the views of the DOE or the U.S. Government. SWCNH synthesis was supported by the University of Trieste, INSTM, the European Commission (H2020 - RIA-CE-NMBP-25 Program, Grant No. 862030), and the Italian Ministry of Education MIUR (cofin Prot. 2017PBXPN4). Part of this work was performed under the Maria de Maeztu Units of Excellence Program from the Spanish State Research Agency Grant No. MDM-2017-0720. Microscopy characterization and Raman measurements were conducted thanks to the Deutsche Forschungsgemeinschaft DFG (Project number 182849149 – SFB 953 Synthetic Carbon Allotropes).

References

1 M. Yudasaka, S. Iijima and V. H. Crespi, *Top. Appl. Phys.: Carbon Nanotubes*, 2008, **111**, 605–629.
2 N. Karousis, I. Suarez-Martinez, C. P. Ewels and N. Tagmatarchis, *Chem. Rev.*, 2016, **116**, 4850–4883.
3 D. Kasuya, M. Yudasaka, K. Takahashi, F. Kokai and S. Iijima, *J. Phys. Chem. B*, 2002, **106**, 4947–4951.

Open Access Article. Published on 23 March 2022. Downloaded on 4/14/2022 6:29:34 PM.
This article is licensed under a Creative Commons Attribution-NonCommercial 3.0 Unported Licence.

4 T. Azami, D. Kasuya, R. Yuge, M. Yudasaka, S. Iijima, T. Yoshitake and Y. Kubo, *J. Phys. Chem. C*, 2008, **112**, 1330–1334.
5 M. Nakamura, Y. Tahara, Y. Ikehara, T. Murakami, K. Tsuchida, S. Iijima, I. Waga and M. Yudasaka, *Nanotechnology*, 2011, **22**, 1–8.
6 K. Ajima, M. Yudasaka, T. Murakami, A. Maigné, K. Shiba and S. Iijima, *Mol. Pharmaceutics*, 2005, **2**, 475–480.
7 B. He, Y. Shi, Y. Liang, A. Yang, Z. Fan, L. Yuan, X. Zou, X. Chang, H. Zhang, X. Wang, W. Dai, Y. Wang and Q. Zhang, *Nat. Commun.*, 2018, **9**, 1–21.
8 M. Zhang, T. Murakami, K. Ajima, K. Tsuchida, A. S. D. Sandanayaka, O. Ito, S. Iijima and M. Yudasaka, *Proc. Natl. Acad. Sci. U. S. A.*, 2008, **105**, 14773–14778.
9 J. Adelene Nisha, M. Yudasaka, S. Bandow, F. Kokai, K. Takahashi and S. Iijima, *Chem. Phys. Lett.*, 2000, **328**, 381–386.
10 T. Itoh, K. Urita, E. Bekyarova, M. Arai, M. Yudasaka, S. Iijima, T. Ohba, K. Kaneko and H. Kanoh, *J. Colloid Interface Sci.*, 2008, **322**, 209–214.
11 E. Bekyarova, K. Murata, M. Yudasaka, D. Kasuya, S. Iijima, H. Tanaka, H. Kahoh and K. Kaneko, *J. Phys. Chem. B*, 2003, **107**, 4681–4684.
12 F. Lodermeyer, R. D. Costa and D. M. Guldi, *Adv. Energy Mater.*, 2017, **7**, 1–19.
13 C. Cioffi, S. Campidelli, C. Sooambar, M. Marcaccio, G. Marcolongo, M. Meneghetti, D. Paolucci, F. Paolucci, C. Ehli, G. M. A. Rahman, V. Sgobba, D. M. Guidi and M. Prato, *J. Am. Chem. Soc.*, 2007, **129**, 3938–3945.
14 R. D. Costa, S. Feihl, A. Kahnt, S. Gambhir, D. L. Officer, G. G. Wallace, M. I. Lucio, M. A. Herrero, E. Vázquez, Z. Syrgiannis, M. Prato and D. M. Guldi, *Adv. Mater.*, 2013, **25**, 6513–6518.
15 F. Lodermeyer, R. D. Costa, R. Casillas, F. T. U. Kohler, P. Wasserscheid, M. Prato and D. M. Guldi, *Energy Environ. Sci.*, 2015, **8**, 241–246.
16 F. Lodermeyer, M. Prato, R. D. Costa and D. M. Guldi, *Nanoscale*, 2016, **8**, 7556–7561.
17 M. Melchionna, M. v. Bracamonte, A. Giuliani, L. Nasi, T. Montini, C. Tavagnacco, M. Bonchio, P. Fornasiero and M. Prato, *Energy Environ. Sci.*, 2018, **11**, 1571–1580.
18 D. Iglesias, A. Giuliani, M. Melchionna, S. Marchesan, A. Criado, L. Nasi, M. Bevilacqua, C. Tavagnacco, F. Vizza, M. Prato and P. Fornasiero, *Chem*, 2018, **4**, 106–123.
19 M. V. Bracamonte, M. Melchionna, A. Giuliani, L. Nasi, C. Tavagnacco, M. Prato and P. Fornasiero, *Sens. Actuators, B*, 2017, **239**, 923–932.
20 K. Urita, S. Seki, S. Utsumi, D. Noguchi, H. Kanoh, H. Tanaka, Y. Hattori, Y. Ochiai, N. Aoki, M. Yudasaka, S. Iijima and K. Kaneko, *Nano Lett.*, 2006, **6**, 1325–1328.
21 J. Suehiro, N. Sano, G. Zhou, H. Imakiire, K. Imasaka and M. Hara, *J. Electrost.*, 2006, **64**, 408–415.
22 Y. Nosho, Y. Ohno, S. Kishimoto and T. Mizutani, *Nanotechnology*, 2006, **17**, 3412–3415.
23 A. Zevalkink, D. M. Smiadak, J. L. Blackburn, A. J. Ferguson, M. L. Chabinyc, O. Delaire, J. Wang, K. Kovnir, J. Martin, L. T. Schelhas, T. D. Sparks, S. D. Kang, M. T. Dylla, G. J. Snyder, B. R. Ortiz and E. S. Toberer, *Appl. Phys. Rev.*, 2018, **5**, 021303.
24 M. Massetti, F. Jiao, A. J. Ferguson, D. Zhao, K. Wijeratne, A. Würger, J. L. Blackburn, X. Crispin and S. Fabiano, *Chem. Rev.*, 2021, **121**, 12465–12547.
25 S. Mauro, *US pat.,* 7125525, 2006.
26 T. Fujimori, K. Urita, Y. Aoki, H. Kanoh, T. Ohba, M. Yudasaka, S. Iijima and K. Kaneko, *J. Phys. Chem. C*, 2008, **112**, 7552–7556.
27 R. Kostić, M. Mirić, T. Radić, M. Radović, R. Gajić and Z. V. Popović, *Acta Phys. Pol., A*, 2009, **116**, 718–721.
28 H. M. Heise, R. Kuckuk, A. Srivastava and B. P. Asthana, *J. Raman Spectrosc.*, 2011, **42**, 294–302.
29 D. Kasuya, M. Yudasaka, K. Takahashi, F. Kokai and S. Iijima, *J. Phys. Chem. B*, 2002, **106**, 4947–4951.
30 C. Thomsen and S. Reich, *Phys. Rev. Lett.*, 2000, **85**, 5214–5217.
31 A. C. Ferrari, *Solid State Commun.*, 2007, **143**, 47–57.
32 D. L. Young, T. J. Coutts, V. I. Kaydanov, A. S. Gilmore and W. P. Mulligan, *J. Vac. Sci. Technol., A*, 2000, **18**, 2978–2985.
33 P. G. Collins, K. Bradley, M. Ishigami and A. Zettl, *Science*, 2000, **287**, 1801–1804.
34 B. Chandra, A. Afzali, N. Khare, M. M. El-Ashry and G. S. Tulevski, *Chem. Mater.*, 2010, **22**, 5179–5183.
35 A. D. Avery, B. H. Zhou, J. Lee, E. S. Lee, E. M. Miller, R. Ihly, D. Wesenberg, K. S. Mistry, S. L. Guillot, B. L. Zink, Y. H. Kim, J. L. Blackburn and A. J. Ferguson, *Nat. Energy*, 2016, **1**, 16033.
36 B. A. MacLeod, N. J. Stanton, I. E. Gould, D. Wesenberg, R. Ihly, Z. R. Owczarczyk, K. E. Hurst, C. S. Fewox, C. N. Folmar, K. Holman Hughes, B. L. Zink, J. L. Blackburn and A. J. Ferguson, *Energy Environ. Sci.*, 2017, **10**, 2168–2179.
37 J. Tan, Z. Chen, D. Wang, S. Qin, X. Xiao, D. Xie, D. Liu and L. Wang, *J. Mater. Chem. A*, 2019, **7**, 24982–24991.
38 Q. Zhang, Y. Sun, W. Xu and D. Zhu, *Energy Environ. Sci.*, 2012, **5**, 9639–9644.
39 N. G. Connelly and W. E. Geiger, *Chem. Rev.*, 1996, **96**, 877–910.
40 J. L. Blackburn, S. D. Kang, M. J. Roos, B. Norton-Baker, E. M. Miller and A. J. Ferguson, *Adv. Electron. Mater.*, 2019, **5**, 1800910.

 This journal is © The Royal Society of Chemistry 2022